Supporting Information for "Tidal strain response of seismic wave velocity at shallow crust in Japan"

Tomoya Takano[1]and Kiwamu Nishida[2]

[1]Graduate School of Science and Technology, Hirosaki University

[2]Earthquake Research Institute, the University of Tokyo

Contents of this file

Introduction

This supporting information contains information on the detail of the state-space model used in this study, the validation of a prior data covariance, the frequency distribution of the velocity change, and the phase delay of velocity changes to the tides.

Text S1. The state vector $\boldsymbol{\alpha}_t$ and the data vector $\boldsymbol{y}_t^p$ for a pth component of correlations ϕ_t^p are defined by,

$$\boldsymbol{\alpha}_t \equiv \begin{pmatrix} A_t \\ \gamma_t \end{pmatrix}, \boldsymbol{y}_t^p \equiv \begin{pmatrix} \phi_t^p\left(\tau_s\right) \\ \vdots \\ \phi_t^p\left(\tau_e\right) \end{pmatrix}, \tag{1}$$

where τ_s is the start of lag time and τ_e is the end of lag time. This study used the lag time from 2 to 15 seconds. $\boldsymbol{R}_t$ is an explanatory variables related to a seismic velocity

———

change caused by the tides. $\boldsymbol{H}_t$ is a diagonal matrix:

$$\boldsymbol{H}_t \equiv h_0 \boldsymbol{I}, \tag{2}$$

where h_0 is a prior data covariance and $\boldsymbol{I}$ is an identity matrix. $\boldsymbol{Q}_t$ also can be written as a diagonal matrix:

$$\boldsymbol{Q}_t \equiv \begin{pmatrix} q_0 & 0 \\ 0 & q_1 \end{pmatrix}, \tag{3}$$

where p_0 and p_1 are a prior model covariance of the amplitude of correlations and stretching parameters, respectively.

Text S2.

The sum of squared residuals between reference and observed noise correlations is not necessarily an appropriate data covariance for the Kalman filter because the model covariance also affects the residual. One possible approach is to estimate h_0 as one of the hyper–parameters by the Maximum Likelihood method. However, it is difficult to stably estimate all hyper-parameters at the same time. We thus first determined p_0, p_1, γ_1, A_{M2}, and ϕ_{M2} by the Maximum Likelihood method with the sum of squared residuals as h_0. By using the determined parameters, we then searched an optimal h_0 by the Maximum Likelihood method with the sum of squared residuals as the initial value of h_0. The estimated h_0 was used to re-determine p_0, p_1, γ_1, A_{M2}, and ϕ_{M2}. Figure S1 shows the logarithmic likelihood as a function of the normalized hyper–parameters with different data covariance. The results were not much different from the hyper–parameters estimated with the sum of squared residuals as data covariance, which is consistent with the consideration of misfit function with unknown data covariance (Dosso & Wilmut, 2006). Therefore, this

study used the sum of squared residuals between reference and observed correlations as data covariance.

Text S3.

Figure S2 shows the frequency distribution of the velocity change at the station where ΔAIC is smaller than 0 and Δ AIC is larger than 0, respectively. At stations where Δ AIC is greater than 0, the velocity change is generally estimated to be smaller than 0.001 %, indicating the tidal response of velocity changes is not statistically significant.

Text S4.

We mapped the phase delay of the seismic velocity variations with respect to the tidal strain (Figure 3 (c)). The phase delay of the velocity variations to the applied strain was potentially caused by the nonlinear elastic response of the rocks (Sens-Schönfelder & Eulenfeld, 2019), such as hysteresis in the rock (Guyer et al., 1995) or slow dynamic recovery after dynamic perturbations (Ostrovsky & Johnson, 2001). The majority of the phase differences observed in this study were approximately 0°. In certain stations, the phase shift reached up to approximately 3 h. The magnitude of this phase shift was consistent with the seismic velocity variations observed in response to the tidal strain with heterogeneous gypcrete in Chile (Sens-Schönfelder & Eulenfeld, 2019). Moreover, several stations exhibited a phase shift of approximately 180°. A phase shift of 180° indicated that the seismic velocity decreased and increased during the contraction and dilatation of the medium, respectively. Although the negative strain–velocity sensitivity can be explained based on the localized fluid movement in the shallow regions owing to tides, the occurrence of such fluid movement could not be verified. Certain stations exhibited negative phase

shifts as well, indicating that the velocity variations delayed the tidal deformation shift by more than 12 h or the velocity variations occurred prior to the deformation. Note that the phase must be off by more than 180 degrees to satisfy causality. Although this study analyzed only the volumetric strain, the orientation of the cracks may govern their strain response in certain directions. In this regard, few studies have discussed the phase delay of velocity variations with respect to the deformation, and the phase lag occurring at the crustal-scale is under discussion. To clarify the phase shifts of the velocity variations with respect to the applied strain, the phase shift mechanisms should be further investigated considering fluid movement and strain orientations.

References

Dosso, S. E., & Wilmut, M. J. (2006). Data uncertainty estimation in matched-field geoacoustic inversion. *IEEE Journal of Oceanic Engineering*, *31*(2), 470–479.

Guyer, R., McCall, K., & Boitnott, G. (1995). Hysteresis, discrete memory, and nonlinear wave propagation in rock: A new paradigm. *Physical review letters*, *74*(17), 3491.

Ostrovsky, L., & Johnson, P. A. (2001). Dynamic nonlinear elasticity in geomaterials. *La Rivista del Nuovo Cimento*, *24*(7), 1–46.

Sens-Schönfelder, C., & Eulenfeld, T. (2019). Probing the in situ elastic nonlinearity of rocks with earth tides and seismic noise. *Physical review letters*, *122*(13), 138501.
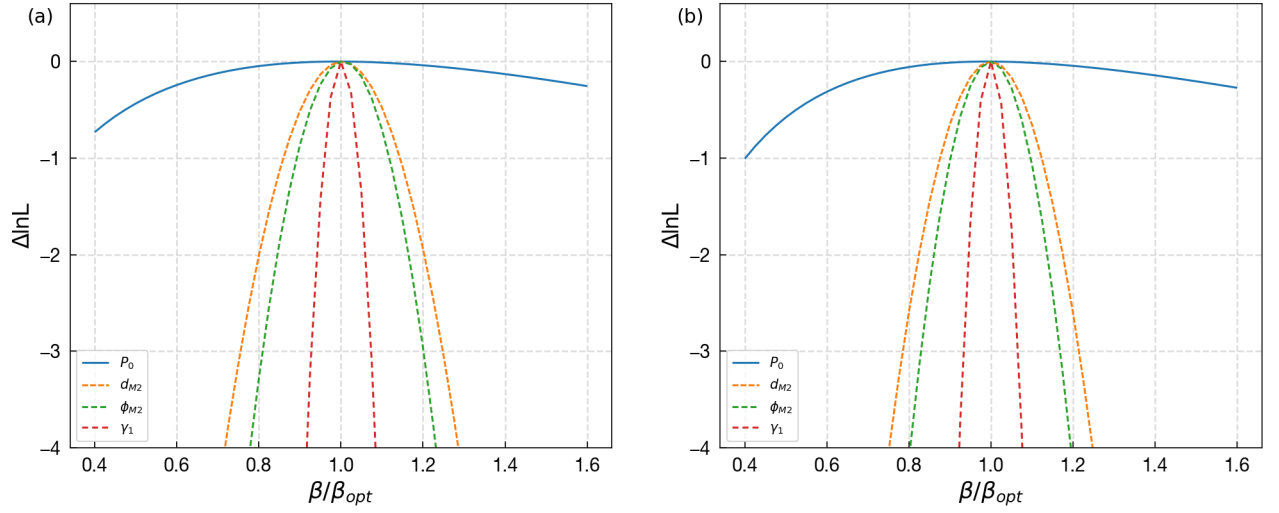
Figure S1. The logarithmic likelihood as a function of the normalized hyper–parameters with the data covariance estimated by the sum of the squared residual between reference and observed correlations (a) and the data covariance estimated by the Maximum likelihood method (b).
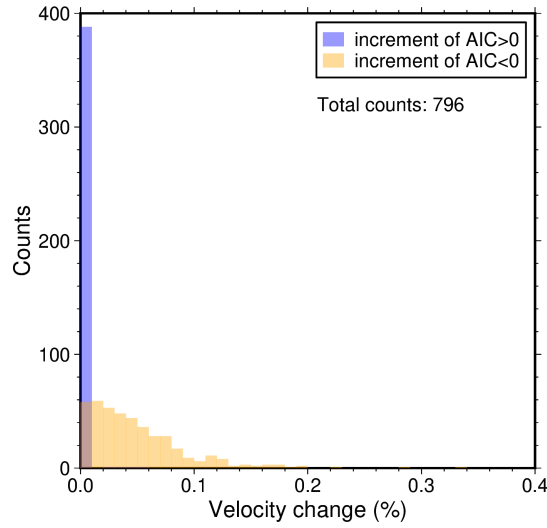

Figure S2. The frequency distribution of velocity changes. Blue bar shows the velocity changes at the stations with increments of AIC larger than 0. Orange bar shows the velocity changes at the stations with increments of AIC smaller than 0.